Bandwidth Allocation for Video Delivery in Wireless Networks with QoE Constraints for Spatially Random User Population

Wei Song and Kai Dong
Faculty of Computer Science
University of New Brunswick
Fredericton, NB, Canada
Emails: {wsong, kdong}@unb.ca

***Abstract*—As video streaming becomes one of the most fast growing and dominant applications in fixed and mobile networks, how to provide high quality and user satisfaction is a widely studied research topic. In this paper, we develop an analytical framework to derive the downloading rate and bandwidth requirement, so that certain objective quality of experience (QoE) constraints are met. Particularly, application-specific key performance indicators (KPIs) such as start-up delay and starvation probability are taken into account. Our analysis addresses heterogeneity of both user spatial locations and video requests. Computer simulations are conducted to verify the accuracy of the proposed analytical framework. Based on the analytical framework, a media server can adapt the downloading rate allocation, e.g., relative to the video playback rate, depending on user demands and network conditions.**

***Index Terms*—Video streaming, QoE, starvation probability, pre-fetching threshold, download-to-playback rate ratio.**

I. Introduction and Related Works

According to Sandvine's global Internet phenomena report, video streaming applications Netflix (31.6%) together with YouTube (18.6%) account for over 50% of downstream traffic on fixed data networks in North America [1]. The most common video delivery is using the hypertext transfer protocol (HTTP) from conventional Web servers given the benefits of fast deployment and network address translation (NAT) traversals. Dynamic adaptive streaming over HTTP (DASH) [2] is one popular HTTP video streaming technique, which can adaptively switch the encoding bit rate of requested video segments to optimize the service quality.

To gauge user satisfaction and acceptance of video services, quality of experience (QoE) becomes a stronger indicator than the traditional quality of service (QoS). As defined in [3], QoE is "the overall acceptability of an application or service, as perceived subjectively by the end-user." Mean opinion score (MOS) is a widely used QoE measure, which is usually expressed in a five-point scale representing different levels of user experience, i.e., *Excellent* (5), *Good* (4), *Fair* (3), *Poor* (2), and *Bad* (1). As subjective assessments for MOS are impractical during service operation, a QoE model that links MOS to objective QoE factors at different layers [4,5] becomes a viable approach to estimate the user-perceived QoE. Many existing QoE models focus on key performance indicators (KPIs) at the network level (e.g., throughput, packet loss, delay, and jitter). Obviously, the key quality indicators (KQIs) at the application level (e.g., start-up delay, freezing interruptions, and picture distortions) can better gauge user satisfaction for video services.

In the literature, there have been many experimental and analytical studies on objective QoE metrics such as starvation probability [6,7], the number of buffer starvations [6], and freezing duration and rate [8]. Here, freezing and starvation mean that the playback buffer at the end user runs below the smallest video decoding block such that the playback is interrupted. Since there is usually a short initial buffering phase before the playback starts, the longer the start-up delay, the larger the amount of pre-fetched video data, and the smoother the playback in general. The trade-off between the start-up delay and the starvation (interruption) probability has been widely explored, e.g., in [6,7]. Such studies often focus on the playback buffer at the receiver, assuming a given or infinite media file length and certain video packet arrival rate to the receive buffer, which largely depends on the network transmission process. In [9], the authors consider both the wireless transmission buffer at the base station and the playback buffer at the end user. However, it assumes an infinite media file length and a fixed number of users with independent and identically distributed (i.i.d.) signal-to-noise ratios (SNRs).

Following a system model similar to [9], we take into account both the wireless transmission process and the playback process. Furthermore, we relax the i.i.d. SNR assumption for end users but consider that the users are randomly deployed in a given area. The spatial distribution of users results in independent but non-identical SNRs, which directly affect the video transmission time and the consequent packet arrival rate to the playback buffer. In addition, we capture the randomness of arrivals and media file lengths of video requests. As a media file is often segmented into chunks that are played

This research was supported in part by Atlantic Canada Opportunities Agency (ACOA) and Mariner Partners.

out for a fixed short interval, the number of video chunks in a video request is assumed to follow a negative binomial distribution, which is a discrete analogue of Gamma distribution. In practice, a media server often allocates a downloading rate to a video request based on the playback rate plus a "small" increment. However, the increment has to be properly calibrated to user demands and network conditions, so that constrains on the start-up delay and starvation probability are satisfied. In this paper, we develop an analytical framework that can determine this serving bandwidth requirement and the small increment over the playback rate. The bandwidth and rate requirements should adapt to user demands and the application-level QoE constraints, e.g., for the start-up delay and starvation probability.

The rest of the paper is organized as follows. Section II presents the system model. In Section III, we introduce an analytical framework to evaluate the video segment arrival rate and the starvation probability. Numerical results are given in Section IV, followed by conclusions in Section V.

II. System Model

A. Video service model

In this work, we focus on the service scenario, where a number of users are streaming videos via the base station (BS) from a multimedia server across the core network. The last-hop wireless links are assumed to be the bottleneck of the end-to-end paths. Using a discrete time scale, we assume that a video request from an end user arrives at the media server with a probability ϑ for each fixed interval Δ. Such a geometric arrival process can be viewed as a discrete-time approximation of the continuous-time Poisson process. For each video request, the corresponding media file has a random playback duration (in seconds), denoted by S. Since the media file is usually composed of video chunks of a fixed playback interval, τ_p, (e.g., 4 seconds), we assume that the number of chunks for each video request (denoted by A) follows a negative binomial distribution, whose probability probability mass function (PMF) is given by

$$\mathrm{P}[A=n] = \binom{n+\nu-2}{n-1}(1-p)^{\nu}p^{n-1} \qquad (1)$$
$$\nu > 0, \quad 0 < p < 1, \quad n = 1, ...$$

where the binomial coefficient

$$\binom{n+\nu-2}{n-1} = \frac{(n+\nu-2)(n+\nu-3)...(\nu)}{(n-1)!}. \qquad (2)$$

The parameters p and ν can be obtained by fitting the mean and variance of the media file length in playback time:

$$\overline{A} = 1 + \frac{\nu p}{1-p}, \qquad \sigma_A^2 = \frac{\nu p}{(1-p)^2}. \qquad (3)$$

The probability generating function (PGF) of A is given by

$$G_A(z) = \sum_{n=1}^{\infty} \mathrm{P}[A=n]z^n = \frac{z(1-p)^{\nu}}{(1-zp)^{\nu}}. \qquad (4)$$

To interpret the physical meaning of p and ν, we can view the number of video chunks in a media file as the outcome of a sequence of independent Bernoulli trials. Given p as the probability of "success" in each trial, the number of successes to observe ν "failures" follows an NB distribution in (1).

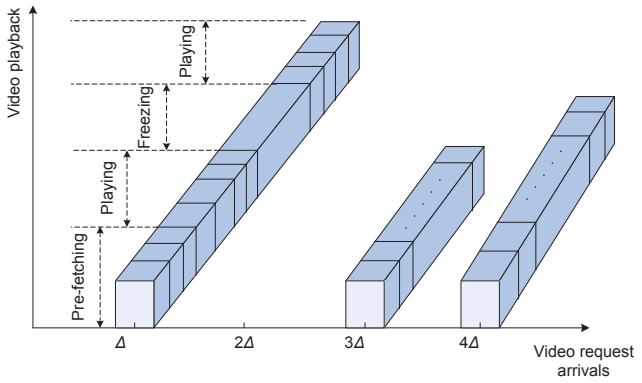

Fig. 1. Video service model.

The video service procedure is depicted in Fig. 1. Upon the arrival of a video request, a batch of video chunks that are generated from the media file will be delivered over a wireless channel via the BS towards the end user. In the initial buffering phase, the video client pre-fetches α chunks (referred to as "pre-fetching threshold") before the playback begins. Taking a video chunk as the smallest decoding block, we assume that the playback is paused when the receive buffer is emptied (starvation). During the freezing period, rebuffering can be initiated to accumulate a minimum amount of data to resume the playing. Here, we are interested in the probability that starvations occur during the playback, which clearly depends on the pre-fetching threshold (α) and the media file length (S), or equivalently the number of chunks in a video request (A).

B. Wireless channel model

To characterize heterogeneity of user channel conditions, we assume that N users are uniformly located in a circular area of a radius L and centered at the BS. Denoting the user intensity by ζ, we have $N = \zeta \cdot \pi L^2$. Further, the wireless channel is assumed subject to Rayleigh fading. The received SNR of a user with a distance r to the BS is then written as

$$\gamma(r) = \bar{\gamma}(r)h(r) = \frac{P_0}{N_0}g(r)h(r) \qquad (5)$$

where $\bar{\gamma}(r)$ is the average received SNR, $h(r)$ represents the small-scale fading which is exponentially distributed with unit mean, $g(r) = r^{-\kappa}$ captures the path loss with a path-loss exponent κ, P_0 is the transmit power, and N_0 is the power of additive white Gaussian noise (AWGN).

Suppose that a user can adaptively select its modulation mode among binary phase-shift keying (BPSK) and square M-ary quadrature amplitude modulation (M-QAM) to match with time-varying channel conditions. Given K modulation modes, the SNR range is partitioned into $(K+1)$ non-overlapping consecutive intervals, with the boundaries denoted by β_k, $k = 0, 1, ...K+1$, where $\beta_0 = 0$ and $\beta_{K+1} = \infty$. The modulation mode k is chosen when $\beta_k \le \gamma < \beta_{k+1}$, so that the bit error rates (BER) satisfies a certain threshold ϵ. The SNR

boundaries β_k ($1 \le k \le K$) can be obtained by evaluating the BER of BPSK and M-QAM as follows:

$$P_{BPSK} = \frac{1}{2}\mathrm{erfc}\left(\sqrt{\frac{E_b}{N_0}}\right) \tag{6}$$

$$P_{QAM} = \frac{4}{b}\left(1 - \frac{1}{\sqrt{M}}\right)\mathrm{Q}\left(\sqrt{\frac{3b}{M-1}\frac{E_b}{N_0}}\right) \tag{7}$$

where M is the constellation size, $b = \log_2 M$, and E_b/N_0 is the ratio of bit energy to noise power intensity. Here, $E_b/N_0 = \gamma \cdot (B_w/R_t)$, where B_w is the channel bandwidth (Hz) and R_t is the rate (bps) of the corresponding modulation.

III. Proposed Analytical Framework

As discussed in Section I, the start-up delay and starvation probability are two important application-level QoE metrics. They depend on the data rate of the wireless channel, spatial locations of users, as well as the video service requests and traffic patterns. In this paper, we develop an analytical framework to characterize the dependence of the objective QoE metrics on the network and service parameters. Following an approach similar to [9], we model the wireless transmission channel and the playback buffer by two queueing systems. The arrival rate of video segments to the playback buffer can be derived by analyzing the queueing model for the wireless transmission channel. Then, we can evaluate the average starvation probability of the spatially random user population, which may request a media file of a random length.

A. Video segment arrival rate

Referring to the video service model in Section II-A, a batch of video segments are queued for transmission over the wireless channel upon a video request arrival. To evaluate the arrival rate of video segments to the playback buffer, we first derive the overall delay to deliver the entire batch. According to the geometric arrivals of video requests, we apply a zero-inflated model [10] to a $D/G/1$ queue, where the inter-arrival time Δ is deterministic. Since a video request arrives in each constant interval Δ with a probability ϑ, we incorporate zero-sized batches with a probability $1-\vartheta$ and a batch size $A \ge 1$ with a probability ϑ. The service time for a video batch follows a general distribution that depends on the number of segments in the batch (i.e., A) and the wireless channel service time for each segment, denoted by Υ. While A follows the NB distribution in (1), Υ varies with the spatial locations of the users and the scheduler applied at the BS.

In this paper, we consider the proportional fairness (PF) scheduler, which is one of the most popular schedulers in cellular networks. PF scheduler can take advantage of multiuser diversity while achieving comparable long-term throughput for all users [11]. Define the relative SNR of user i as the ratio of the instantaneous SNR to average SNR, given by $x_i = \frac{\gamma_i}{\bar{\gamma}_i}$, $i = 1, 2, ..., N$. Then, the relative SNR of the user selected by the PF scheduler for transmission is expressed as

$$X = \max\left\{\frac{\gamma_1}{\bar{\gamma}_1}, \frac{\gamma_2}{\bar{\gamma}_2}, ..., \frac{\gamma_N}{\bar{\gamma}_N}\right\} \triangleq \frac{\Gamma^*}{\overline{\Gamma}}. \tag{8}$$

Here, $\overline{\Gamma}$ is a random variable of the average SNR values of N users, while Γ^* denotes the SNR of the selected user. Based on the fading model in (5), since $\frac{\gamma_i}{\bar{\gamma}_i}$ follows an exponential distribution of unit mean, the cumulative distribution function (CDF) of X can be easily obtained as

$$\mathrm{P}\big[X \le x\big] = \big(1 - e^{-x}\big)^N. \tag{9}$$

To derive the distribution of Γ^*, which directly affects the selection of modulation mode and transmission rate, we first analyze the distribution of $\overline{\Gamma}$. Considering the heterogeneous scenario depicted in Section II-B, the average SNR varies with the location-dependent path loss. We focus on a circular ring area centered at the BS of an inner radius δ and an outer radius L. That is, a very small circular area of a radius δ is excluded for analysis tractability. Thus, the CDF of $\overline{\Gamma}$ is written as

$$\mathrm{P}\big[\overline{\Gamma} \le y\big] = \mathrm{P}\left[\frac{P_0}{N_0} r^{-\kappa} \le y\right] = \mathrm{P}\left[r \ge \left(\frac{P_0/N_0}{y}\right)^{1/\kappa}\right]. \tag{10}$$

When the users are uniformly distributed in the ring area, the CDF of user distance to the center BS (R) is given by

$$\mathrm{P}\big[R \le r\big] = \frac{r^2 - \delta^2}{L^2 - \delta^2}, \quad \delta \le r \le L. \tag{11}$$

Hence, we have

$$\begin{aligned}\mathrm{P}\big[\overline{\Gamma} \le y\big] &= \mathrm{P}\left[\left(\frac{P_0/N_0}{y}\right)^{1/\kappa} \le R \le L\right] \\ &= \frac{\left(\frac{P_0/N_0}{y}\right)^{2/\kappa} - \delta^2}{L^2 - \delta^2} \triangleq F(y).\end{aligned} \tag{12}$$

The CDF of Γ^* is then derived by

$$\begin{aligned}\mathrm{P}\big[\Gamma^* \le u\big] &= \mathrm{P}\Big[X \le \frac{u}{\overline{\Gamma}}\Big] \\ &= \int_{\bar{\gamma}_{\min}}^{\bar{\gamma}_{\max}} \big(1 - e^{-\frac{u}{y}}\big)^N F'(y)\, dy\end{aligned} \tag{13}$$

where $\bar{\gamma}_{\min} = (P_0/N_0)L^{-\kappa}$, $\bar{\gamma}_{\max} = (P_0/N_0)\delta^{-\kappa}$, and $F'(y)$ is the probability density function (PDF) of $\overline{\Gamma}$.

As a modulation mode k ($1 \le k \le K$) is employed when the received SNR falls within a range $[\beta_k, \beta_{k+1})$. Hence, the probability that the user selected by the PF scheduler uses modulation mode k is given by

$$\begin{aligned}p_k &= \mathrm{P}\big[\Gamma^* \le \beta_{k+1}\big] - \mathrm{P}\big[\Gamma^* \le \beta_k\big] \\ &= \int_{\bar{\gamma}_{\min}}^{\bar{\gamma}_{\max}} \big(1 - e^{-\frac{\beta_{k+1}}{y}}\big)^N F'(y)\, dy \\ &\quad - \int_{\bar{\gamma}_{\min}}^{\bar{\gamma}_{\max}} \big(1 - e^{-\frac{\beta_k}{y}}\big)^N F'(y)\, dy.\end{aligned} \tag{14}$$

Let τ_s denote a transmission timeslot. Given it takes η_k timeslots to transmit a video segment with modulation mode k, we obtain the PGF of channel service time as

$$G_T(z) = p_1 z^{\eta_1} + p_2 z^{\eta_2} + \cdots + p_K z^{\eta_K}. \tag{15}$$

The PGF of the service time for an entire batch of video segments of a media file is then given by

$$G_B(z) = \sum_{n=1}^{\infty} \mathrm{P}[A=n] \sum_{k=1}^{\infty} \mathrm{P}[T_1 + ... + T_n = k | A = n] z^k$$
$$= \sum_{n=1}^{\infty} \mathrm{P}[A=n] \cdot [G_T(z)]^n = G_A(G_T(z)) \quad (16)$$

where $G_A(\cdot)$ and $G_T(\cdot)$ are given by (4) and (15), respectively. Considering the zero-inflated model to account for geometric arrivals of video requests, (16) is modified as follows:

$$\widetilde{G}_B(z) = (1-\vartheta) + \vartheta G_B(z). \quad (17)$$

Then, using the approach in [12], we obtain the PGF of the time to transmit an entire batch of video segments, given by

$$W(z) = \frac{\Phi \cdot (z-1) \prod_{j=1}^{J-1} (z - z_j)}{z^J - \widetilde{G}_B(z)} \quad (18)$$

where $J = \Delta/\tau_s$, z_1, ..., z_{J-1} are the unique roots of $z^J - \widetilde{G}_B(z) = 0$ within the unit circle $|z| < 1$, and Φ is a normalization constant. Based on (18), the mean time to transmit all video segments of a media file is obtained as

$$\overline{W} = -\frac{J(J-1) - \widetilde{G}''_B(1^-)}{2[J - \widetilde{G}'_B(1^-)]} + \sum_{j=1}^{J-1} \frac{1}{1-z_j} \quad (19)$$

where $\widetilde{G}'_B(1^-)$ and $\widetilde{G}''_B(1^-)$ are the left-hand limit of the first-order and second-order derivatives of $\widetilde{G}_B(z)$ at 1^-, respectively. The average arrival rate of video segments to the playback buffer is given by $\lambda = \overline{A}/\overline{W}$ (video segments per slot τ_s).

B. Pre-fetching threshold and starvation probability

As in [6,7], we consider an $M/D/1$ queueing model for the playback buffer. That is, the video segments are delivered over the wireless channel and arrive at the playback buffer as a Poisson process. Since the media file is decomposed into video segments of a fixed playback interval τ_p, only one video segment is served by the playback queue per interval τ_p. Given α video segments are pre-fetched before the playback starts, the starvation probability for a media file consisting of n segments in total is obtained as [6]

$$P_s(\alpha, n) = \sum_{l=\alpha}^{n-1} \frac{\alpha}{l} \frac{(\tilde{\lambda} l)^{l-\alpha}}{(l-\alpha)!} e^{-\tilde{\lambda} l} \quad (20)$$

where $\tilde{\lambda} = \lambda \tau_p / \tau_s$, which is the average segment arrival rate per playback interval τ_p, $\tilde{\lambda} l$ is then the average number of segment arrivals in l playback intervals, and $\frac{(\tilde{\lambda} l)^{l-\alpha}}{(l-\alpha)!} e^{-\tilde{\lambda} l}$ is the probability that there are $(l-\alpha)$ segment arrivals in l playback intervals according to the Poisson arrival process.

When $n \to \infty$, it is difficult to calculate the righthand side of (20). Hence, we use the following Gaussian approximation when n is sufficiently large (no less than a large threshold Λ):

$$P_s(\alpha, n) \approx \sum_{l=\alpha}^{\Lambda-1} \frac{\alpha}{l} \frac{(\tilde{\lambda} l)^{l-\alpha}}{(l-\alpha)!} e^{-\tilde{\lambda} l} + \int_{\Lambda}^{n-1} \frac{\alpha}{l} \frac{1}{\sqrt{2\pi \tilde{\lambda} t}} \exp\left(\frac{\left(t - \alpha - \tilde{\lambda} t\right)^2}{2\tilde{\lambda} t} \right) dt. \quad (21)$$

Since the media file length is assumed to follow the NB distribution in (1), the average starvation probability among the users is then given by

$$\overline{P}_s(\alpha) = \sum_{n=1}^{\infty} \mathrm{P}[A=n] P_s(\alpha, n)$$
$$= \sum_{n=1}^{\infty} \binom{n+\nu-2}{n-1} (1-p)^{\nu} p^{n-1} \sum_{l=\alpha}^{n-1} \frac{\alpha}{l} \frac{(\tilde{\lambda} l)^{l-\alpha}}{(l-\alpha)!} e^{-\tilde{\lambda} l}. \quad (22)$$

As the start-up delay is directly proportional to the pre-fetching threshold α, it is necessary to limit $\alpha \leq \sigma$ to upper bound the start-up delay. Based on (22), the minimum required video segment arrival rate $\tilde{\lambda}$ can be derived to guarantee $\overline{P}_s(\sigma) \leq \omega$, where ω represents the QoE constraint (e.g., 1%). The video segment arrival rate $\tilde{\lambda}$ is actually the downloading rate via the wireless channel. According to the analysis in Section III-A, we can further derive the bandwidth requirement to achieve the required downloading rate. Here, we express the average downloading rate relative to the average playback rate (referred to as download-to-playback rate ratio) as $\varphi = (\overline{A}\tau_p)/(\overline{W}\tau_s)$.

TABLE I
SYSTEM PARAMETERS.

Definition	Symbol	Value
Transmit SNR	P_0/N_0	45 $\sim$ 55 dB
Minimum distance to BS	δ	0.5 m
Maximum distance to BS	L	100 $\sim$ 1000 m
Path loss exponent	κ	2.5
User intensity per unit area (m^2)	ζ	5×10^{-5}
BER requirement	ϵ	10^{-5}
Playback interval	τ_p	4 s
Video request arrival probability	ϑ	0.1 $\sim$ 0.2
Mean of number of video segments	$\overline{A}$	30
Variance of number of video segments	σ_A^2	45

IV. NUMERICAL AND SIMULATION RESULTS

In this section, we verify the accuracy of the analytical framework in Section III and demonstrate how the video segment arrival rate and starvation probability vary with the system parameters. Both the numerical analysis and computer simulations are conducted with MATLAB 7.14.0 (R2012a). The system parameters are given in Table I.

Based on the analysis in Section III-A, we can obtain the average arrival rate of video segments to the playback buffer. This segment arrival rate is directly related to the wireless

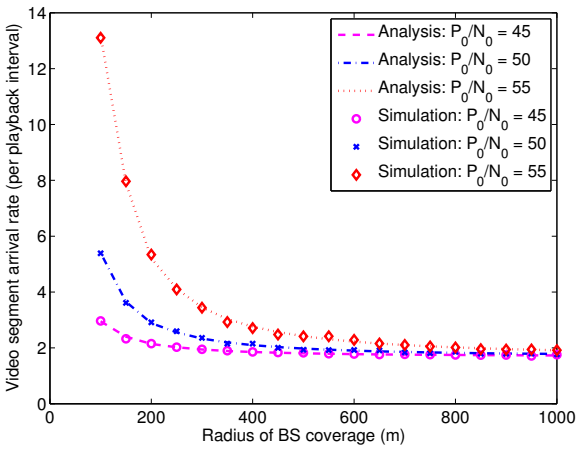

Fig. 2. Average arrival rate of video segments $\tilde{\lambda}$ (per playback interval τ_p) vs. radius of BS coverage area L with varying transmit SNRs P_0/N_0.

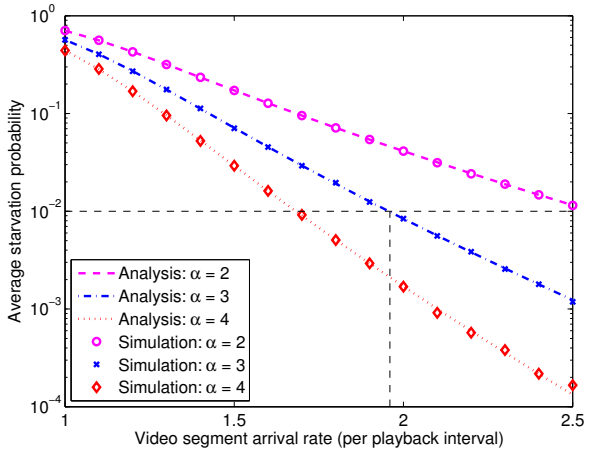

Fig. 3. Average starvation probability $\overline{P}_s$ vs. average arrival rate of video segments $\tilde{\lambda}$ (per playback interval τ_p) with varying pre-fetching thresholds α.

channel service rate, which depends on the network topology and transmission parameters. Fig. 2 shows the analysis and simulation results against the radius of BS coverage (L) and transmit SNR (P_0/N_0). As seen, the analysis results match well the simulation results. It is also observed that the video segment arrival rate decreases exponentially with L when $L \leq 200$. This is due to the adaptive modulation based on the received SNR, which depends on the transmitter-receiver distance as well as the transmit SNR. When the distance together with the transmit SNR result in the selection of higher-rate modulation modes, there can be a larger arrival rate of video segments. In contrast, when the distance becomes large enough, the lowest modulation mode is always chosen and the consequent video segment arrival rate only varies slightly.

Further considering the heterogeneity of user video requests, we can evaluate the average starvation probability $\overline{P}_s(\alpha)$ for a given pre-fetching threshold α. The pre-fetched α video segments during initial buffering can sustain continuous playback of a duration $\alpha\tau_p$ by itself. To verify the accuracy of the analysis in Section III-B, Fig. 3 shows the average starvation probability versus the average video segment arrival rate with different pre-fetching thresholds. It is clearly seen that the analysis results are very accurate. Moreover, it is found that the starvation probability exponentially degrades with the video segment arrival rate, since a log-scale is applied in the y-axis. Based on the analysis, we can easily obtain the minimum required video segment arrival rate to satisfy a QoE constraint on the starvation probability, given an upper bound of the pre-fetching threshold. As illustrated by the dashed black lines in Fig. 3, the minimum required arrival rate to ensure $\overline{P}_s \leq 1\%$ and $\alpha \leq 3$ is 1.96 video segments per playback interval.

V. Conclusions

Start-up delay and starvation probability are two important objective QoE metrics for video streaming and their trade-off has been widely explored. In this paper, we further take into account heterogeneity of spatial distributions and video requests of end users in the proposed analytical framework. Specifically, the received SNRs are considered exponentially distributed with different location-dependent means. The media file length or, equivalently, the number of video chunks in a video request, is assumed to follow a negative binomial distribution. We can accurately evaluate the starvation probability, which depends on the pre-fetching threshold and the video downloading rate. Based on the analytical framework, the media server can dynamically adjust the bandwidth and downloading rate allocation, e.g., relative to the video playback rate, to ensure consistent quality and minimum bandwidth wastage.

References

[1] Sandvine, "Sandvine report: Netflix and YouTube account for 50% of all North American fixed network data," 2013.

[2] T. Stockhammer, "Dynamic adaptive streaming over HTTP: Standards and design principles," in *Proc. ACM Conference on Multimedia Systems*, 2011, pp. 133–144.

[3] ITU-T, "ITU-T Recommendation G.100/P.10, Vocabulary for performance and quality of service, Amendment 2: New definitions for inclusion in Recommendation P.10/G.100," 2008.

[4] P. Rengaraju, C.-H. Lung, F. R. Yu, and A. Srinivasan, "On QoE monitoring and E2E service assurance in 4G wireless networks," *IEEE Wireless Commun. Mag.*, vol. 19, no. 4, pp. 89–96, 2012.

[5] P. Reichl, B. Tuffin, and R. Schatz, "Logarithmic laws in service quality perception: Where microeconomics meets psychophysics and quality of experience," *Telecommunication Systems*, vol. 52, no. 2, pp. 587–600, 2013.

[6] Y. Xu, E. Altman, R. E. Azouzi, M. Haddad, S.-E. Elayoubi, and T. Jiménez, "Analysis of buffer starvation with application to objective QoE optimization of streaming services," *IEEE Trans. Multimedia*, vol. 16, no. 3, pp. 813–827, 2014.

[7] A. ParandehGheibi, M. Méard, A. E. Ozdaglar, and S. Shakkottai, "Avoiding interruptions - A QoE reliability function for streaming media applications," *IEEE J. Select. Areas Commun.*, vol. 29, no. 5, pp. 1064–1074, 2011.

[8] L. Chen, Y. Zhou, and D. M. Chiu, "Smart progressive downloading," *CoRR - Computing Research Repository*, vol. abs/1307.4581, 2014.

[9] Y. Xu, E. Altman, R. El-Azouzi, S. E. Elayoubi, and M. Haddad, "QoE analysis of media streaming in wireless data networks," *Lecture Notes in Computer Science - NETWORKING 2012*, vol. 7290, pp. 343–354, 2012.

[10] N. Jansakul and J. P. Hinde, "Score tests for extra-zero models in zero-inflated negative binomial models," *Communications in Statistics - Simulation and Computation*, vol. 38, no. 1, pp. 92–108, 2009.

[11] J. G. Andrews, A. Ghosh, and R. Muhamed, *Fundamentals of WiMAX: Understanding Broadband Wireless Networking*. Prentice Hall, 2007.

[12] L. D. Servi, "D/G/1 queues with vacations," *Operations Research*, vol. 34, no. 4, pp. 619–629, 1986.